La mer 35: 15–22, 1997
Société franco-japonaise d'océanographie, Tokyo

A three-dimensional numerical model of tide and tidal current in the Gulf of Tongking

Dinh-Van MANH* and Tetsuo YANAGI*

Abstract: On the basis of the finite defference method and the vertically σ-stretched transformation, a 3-D numerical model is established to calculate the tide and the tidal current as well as the tide-induced residual flow in the Gulf of Tongking. The model is calibrated by using the data at the tide gauge stations as well as from satellite observation. The most important tidal characteristics of 4 major constituents K_1, O_1, M_2, and S_2 are reproduced well. Next the tide-induced residual flows due to K_1 and M_2 tides are calculated. The strongest residual flow of about 10 cm/s in the case of K_1 tide occurs in the south-west coastal zone of Hai-Nan Island.

1. Introduction

The Gulf of Tongking, situated between Hai-Nan Island of China and the north coast of Vietnam, is one of the two largest gulfs in the South China Sea. This is a rather shallow sea area with the average depth of about 45m and the maximum one of 100m at the mouth (Fig. 1). It is known that the tidal regime is diurnal nearly in the whole gulf (HUANG *et al.*, 1994). The tidal amplitude is changed noticeably and the largest one reaches 2.5m at the head of the gulf.

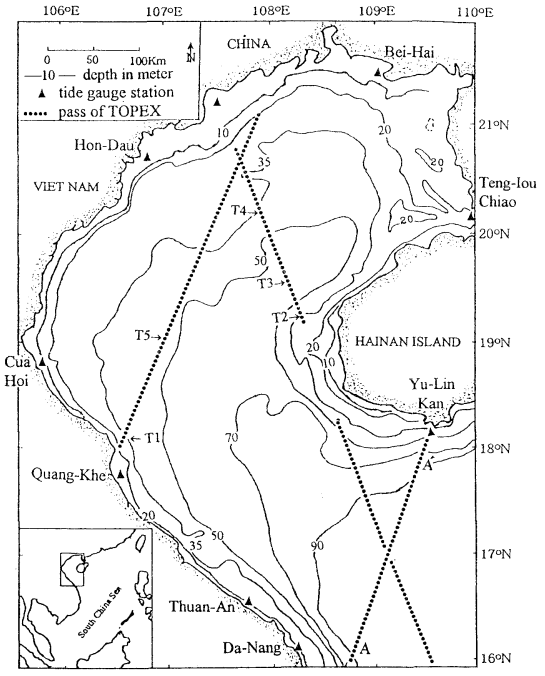

Fig. 1. Geometry of the Gulf of Tongking and the observed data locations.

Up to now some studies on the numerical simulation of tide in the South China Sea as well as in the gulf of Tongking have been carried out (THUY, 1969; HUANG *et al.*, 1994). In these studies the elliptical equation system without friction term or the 2-D horizontal shallow water equations were solved, therefore the vertical structure of tidal currents has not been revealed yet.

In this paper, a 3-D numerical model based on the 3-D Saint Vernant equation system (NIHOUL and JAMART, 1987) is used to simulate the propagation of tidal wave as well as to consider the tidal currents and the tide-induced residual flow in the Gulf of Tongking.

2. Governing equations and solving procedure

It is common in tidal models to make some simplifying approximations in the equations of fluid motion. The fluid is assumed to be incompressible. The vertical momentum equation can be approximated by the hydrostatic pressure equation, that is a hydrostatistic approximation. With these assumptions, the continuity equation and the horizontal momentum

*Department of Civil and Ocean Engineering
Ehime University, Matsuyama 790, Japan

equations take the following forms :

$$\frac{\partial u}{\partial x}+\frac{\partial v}{\partial y}+\frac{\partial w}{\partial z}=0 \tag{1}$$

$$\frac{\partial u}{\partial t}+\frac{\partial (uu)}{\partial x}+\frac{\partial (uv)}{\partial y}+\frac{\partial (uw)}{\partial w}-\Omega v = -g\frac{\partial \zeta}{\partial x}+A_h\frac{\partial^2 u}{\partial x^2}+A_h\frac{\partial^2 u}{\partial y^2}+\frac{\partial}{\partial z}\left(A_v\frac{\partial u}{\partial z}\right) \tag{2}$$

$$\frac{\partial u}{\partial t}+\frac{\partial (vu)}{\partial x}+\frac{\partial (vv)}{\partial y}+\frac{\partial (vw)}{\partial w}-\Omega u = -g\frac{\partial \zeta}{\partial y}+A_h\frac{\partial^2 v}{\partial x^2}+A_h\frac{\partial^2 v}{\partial y^2}+\frac{\partial}{\partial z}\left(A_v\frac{\partial v}{\partial z}\right) \tag{3}$$

Here x, y, z is a Cartesian coordinate with the z axis pointing vertically upwards and the xy-plane being the undisturbed position of the water surface. u, v, w are x, y, z velocity components, respectively ; $\zeta(x, y, t)$, height of the water surface above the mean sea surface; Ω, Coriolis parameter ($=2\omega\sin\phi$, ω is the angular velocity of rotation of the earth ; ϕ is latitude); g ($=980\text{cm/s}^2$), the acceleration due to gravity ; and A_v, A_h, vertical and horizontal eddy viscosities, respectively.

In addition to the above equations, there are boundary conditions at the sea surface $z=0$, at the bottom $z=-h$, and at the lateral boundaries. They are

$$\text{at } z=0 : \frac{\partial \zeta}{\partial t}+u\frac{\partial \zeta}{\partial x}+v\frac{\partial \zeta}{\partial y}-w=0, \tag{4}$$

$$\rho A_v\frac{\partial u}{\partial x}=0, \quad \rho A_v\frac{\partial u}{\partial z}=0 \tag{5}$$

$$\text{at } z=-h : u\frac{\partial h}{\partial x}+v\frac{\partial h}{\partial y}+w=0 \tag{6}$$

$$\rho A_v\frac{\partial u}{\partial z}=\tau_x^b, \quad \rho A_v\frac{\partial v}{\partial z}=\tau_y^b \tag{7}$$

At the solid boundary: The velocity component normal to this boundary is suppressed :

$$V_n=0, \ (\vec{n} \text{ is the unit outward vector}) \tag{8}$$

At the open boundry: The sea water level is prefixed on the basis of observational results :

$$\zeta=f(x, y, t) \tag{9}$$

The vertical viscosity A_v, according to the Prantl's mixing length theory, is taken as

$$A_v=A_{v0}+l^2\sqrt{(\partial u/\partial z)^2+(\partial v/\partial z)^2}, \quad l=k_0(z+h+z_0)[1-(z+h)/h)] \tag{10}$$

where k_0 ($=0.4$) is the Karman constant ; z_0 ($=10\text{cm}$) is the sea bed roughness length ; A_{v0} is a small number to prevent the case of dividing by zero during the calculation.

The components of bottom friction stress (τ_x^b, τ_y^b) are got the following form :

$$(\tau_x^b, \ \tau_y^b)=\beta\sqrt{(u^2+v^2)}(uv) \tag{11}$$

where β is the bottom friction coefficient ($=0.026$).

In order to solve the above mentioned equation system to determine velocity components as well as sea water level, the finite defference method is applied. Some parameters of the numerical model are taken as : the horizontal space steps equal to 1/6 degrees ; the number of layers is 6 ; the horizontal eddy viscosity, $A_h=10^6\text{cm}^2/\text{s}$. The solving procedure at each time step is described as follows :

Firstly, the depth averaged velocity components and sea water levels are determined. By integrating the above equations over the range from $z=-h$ to $z=\zeta$ and using the boundary conditions of(4) to (7), the modified shallow water equations are obtained. These equations with the boundary conditions can be solved by one of the existing two dimensional algorithms, and in this computation an alternative direction implicit (ADI) Scheme (RAMMING and KOWALIK, 1980) is employed.

Secondly, for 3-D velocity components computation, a vertically σ-stretched grid (NIHOUL and JAMART, 1987) is applied with $\sigma=(z+h)/(h+\zeta)$ and hence σ varies between 0 and 1. Therefore the spacing steps on each vertical grid line are regular and the accuracy of bathymetry approximation is improved. Using the depth mean velocity components and sea water levels determined in the first stage, as well as the boundary conditions of (5) and (7) the equations of (2) and (3) are approximated by a finite difference scheme, implicit in the vertical direction and explicit in the horizontal ones (LARDNER, 1988), in order to get a pair of recursive formulae on each vertical grid line

$u_{j+1}=R_ju_j+S_jv_j+Q_j^x$, $v_{j+1}=S_jv_j+R_ju_j+Q_j^x$

where j denotes the jth vertical grid level. Coefficients R_j, S_j, $Q_j{}^x$, $Q_j{}^y$ are computed recursively downwards from j=N ($z=\zeta$) to $j=1$ ($z=-h$). Then the horizontal velocity components u_j, v_j are computed recursively upwards from j

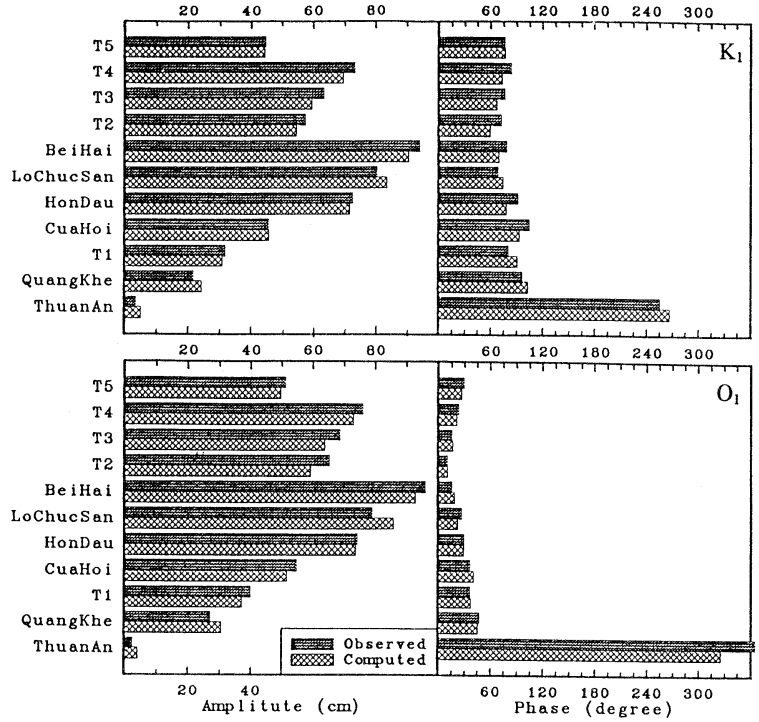

Fig. 2. The observed data and computed results of K_1 tide(above)and O_1 tide(below)at the stations.

$=1$ to $j=N$.

Lastly, the vertical velocity component is obtained by integrating the equation (1) from bottom to surface.

It is known that tide-induced residual flow plays an important role in the long-term transport of substances. It may be obtained by averaging the tidal current over one tidal cycle.

3. Results

Data used for the open sea boundary condition and the model calibration are the harmonic constants of 4 major constituents K_1, O_1, M_2, S_2 at the tide gauge stations and from satellite observation, TOPEX (YANAGI *et al.* 1997). At the open sea boundaries, the sea surface oscillations due to each of the above mentioned constituents are given by using the data along the AA' pass of TOPEX and at 3 tide gauge stations Da-Nang, Yu-Lin-Kan and Teng-Iou-Chiao. The data at 6 other stations and 5 points, denoted by T1,··· T5, of TOPEX are employed for the calibration. Among these, Cua-Hoi, Hon-Dau and Bei-Hai are 3 standard tide gauge stations. The data locations are shown in Fig. 1.

a. Diurnal Tides:

The comparison between the calculated results and the observed data of two diurnal tides K_1 and O_1 are presented in Fig. 2. For K_1 tide, the maximum absolute error of amplitude is less than 4 cm (6.2%), and of phase is 13.5° (54 minutes). In the case of O_1 tide, the error of amplitude is larger, reaches 6.7cm(8.5%), but the errors of phase is smaller, not exceed 5° (20 minutes), except at Thuan-An.

The amplitude and phase distributions of these constituents obtained from the numerical model are displayed in Fig. 3. An amphidromic point exists near the Thuan-An in both two cases. Tidal amplitude increases gradually in the south-north direction and gets the maximum value, greater than 80cm, at the head of the gulf. Tidal ellipses of K_1 constituent at three layers ; the upper(−5m), middle(−20m) and lower layers (−50m), are expressed in Fig. 4. The predominant direction of tidal currents is parallel to the shoreline. The strongest

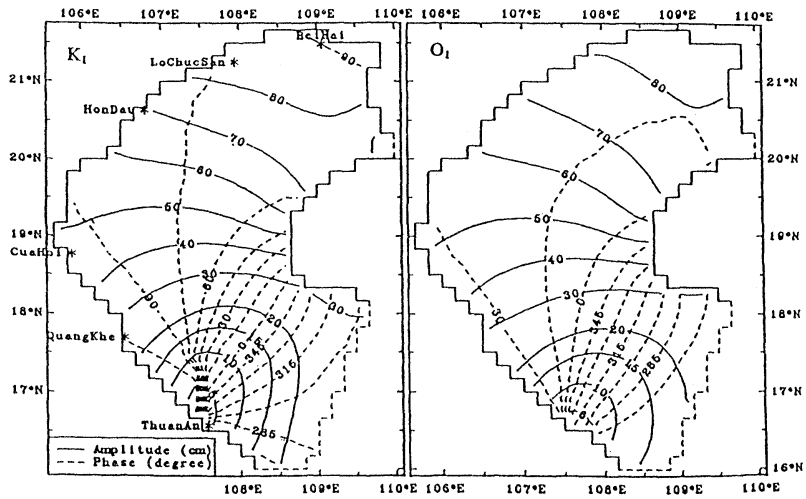

Fig. 3. The calculated co-range and co-phase charts of K_1 tide(left)and O_1 tide (right).

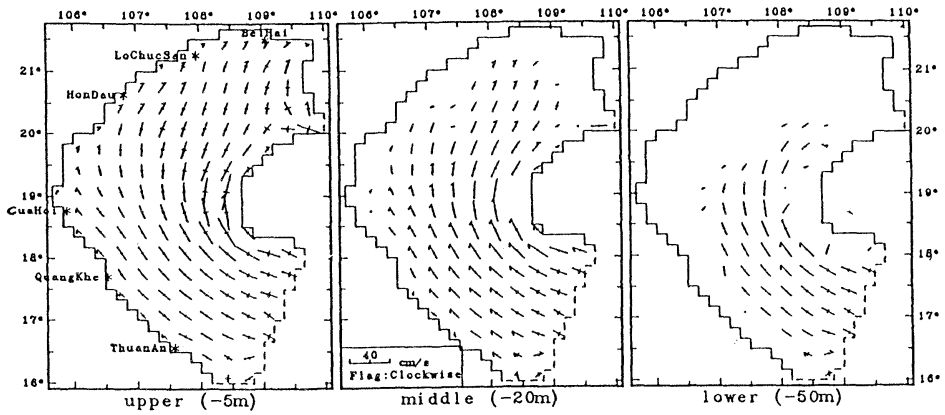

Fig. 4. The calculated tidal ellipses of K_1 tide at three layers.

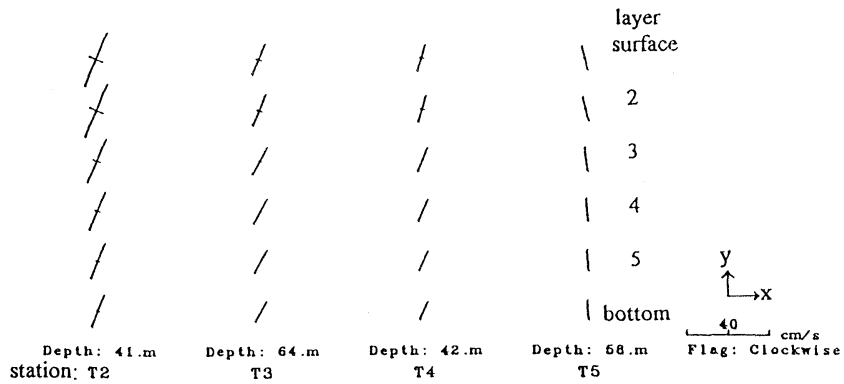

Fig. 5. The calculated tidal ellipses of K_1 tide in the vertical direction at some points.

currents (reach 60cm/s) occur in the southwest coastal zone of Hai-Nan Island. The rotational direction of tidal ellipse is mainly clockwise. The major axes of tidal ellipses rotate slightly in clockwise direction downwards as shown in Fig. 5. The comparison between

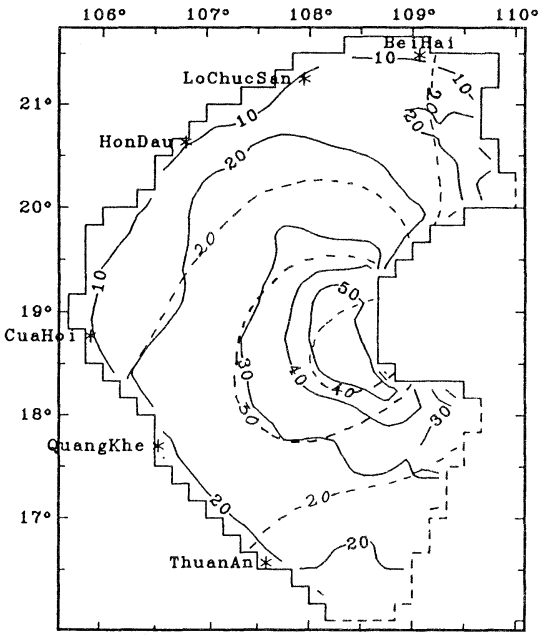

Fig. 6. The Maximum current velocity distributions of K_1 constituent.
----observed (FANG, 1986), ——calculated.

the observed distribution of maximum current velocity
(FANG, 1986) and the calculated one shows that the calculated currents well reproduce to the observed data in quantity as shown in Fig. 6. The O_2 tidal ellipses are similar to the K_1 ones (not presented here).

b. Semi-Diurnal Tides :

Figure 7 presents the amplitudes and phases of M_2 and S_2 tidal waves from observation as well as the model results. It is shown that the model results agree with the observed data. In the case of M_2, the maximum absolute error in amplitude is 3cm (32%) at T2, and in phase is 22° (45 minutes) at Thuan-An. For S_2 tide, with the amplitude about 2 times smaller than M_2, the phase errors at almost stations are a little greater (up to 24°).

The amplitude and phase distributions of semi-diurnal tides are presented in Fig. 8. The maximum amplitude region is the northeastern part of the gulf. However, there is another region having relatively large tidal amplitude, around Cua-Hoi. The amplitude near Hon-Dau

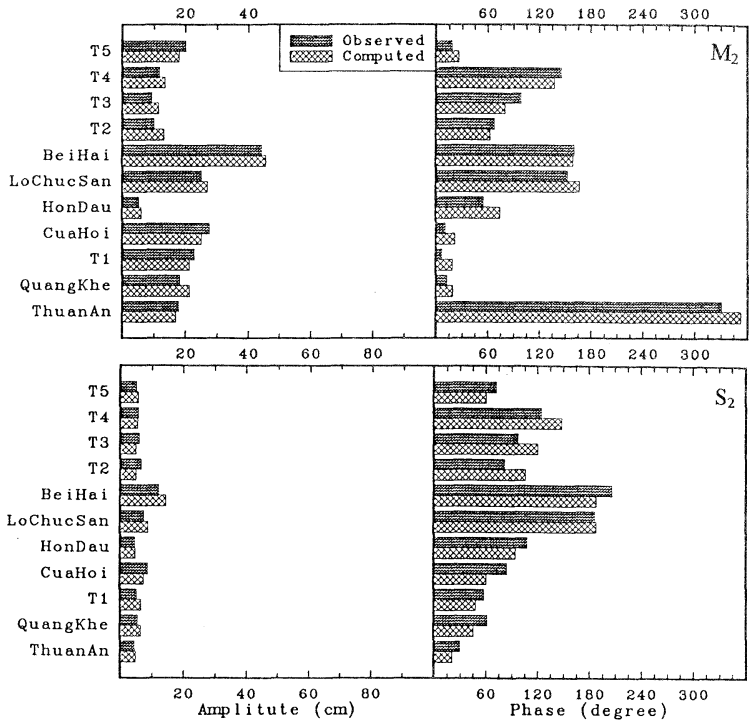

Fig. 7. The observed data and computed results of M_2 tide(above)and S_2 tide(below)at the stations.

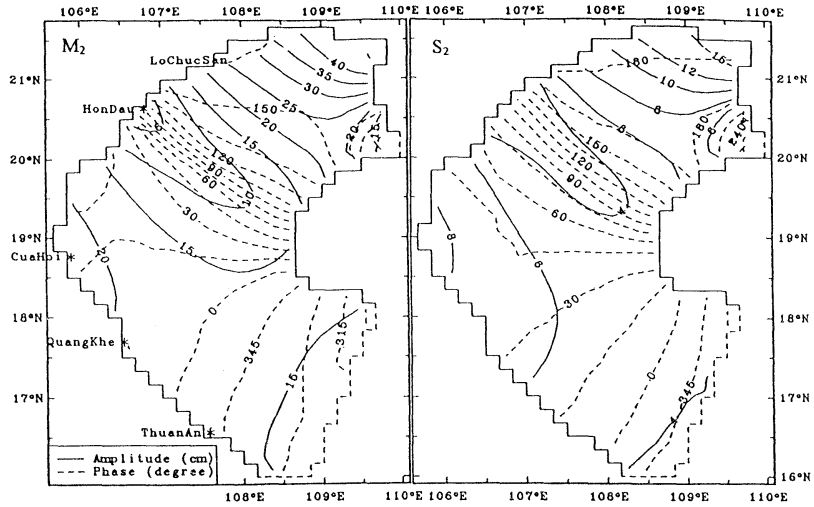

Fig. 8. The calculated co-range and co-phase charts of M_2 tide (left) and S_2 tide (right).

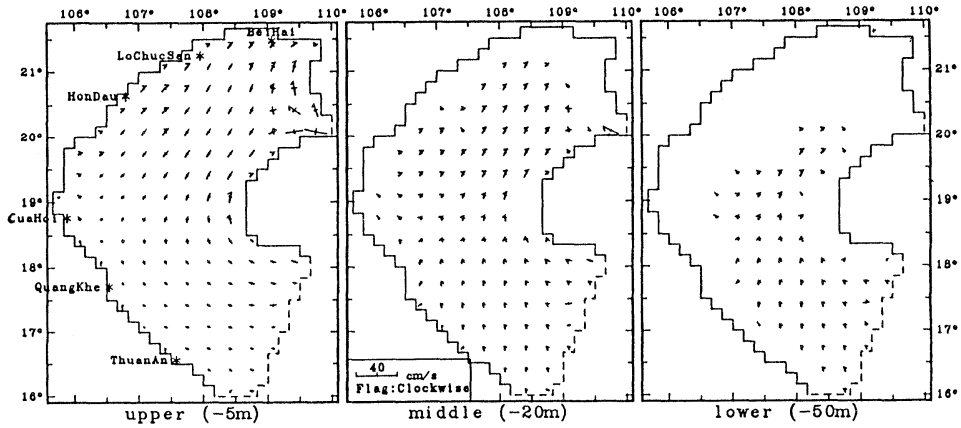

Fig. 9. The calculated tidal ellipses of M_2 tide at three layers.

region decreases. In Fig. 9 the tidal current ellipses of M_2 constituent are shown. In this case the tidal currents mainly rotate in the counter-clockwise direction. The S_2 tidal currents have the similar pattern to the M_2 ones but smaller in magnitude.

c. Tide-induced residual flows

The tide-induced residual flows are calculated in two cases, those due to K_1 tide and M_2 tide. The residual flows at three layers due to K_1 tide are displayed in Fig. 10. It is shown that the strongest flow of about 10cm/s occurs at the middle layer in the south-west coastal zone of Hai-Nan Island, where the K_1 tidal currents are the strongest. Another region with the considerable strong flow is the coastal zone from Thuan-An to Quang-Khe of Vietnam. In the northwestern part of the gulf the flow speed is small. There is a large anti-clockwise eddy with the center located at 107° 50'E and 18° 10'N. Besides, some other small eddies exist in the northern part of the gulf. The M_2 tide causes a weaker residual flow. The remarkable residual flow due to M_2 tide is along the shore from Hai-Nan Strait to Thuan-An. The flow is quite small offshore and in the coast zone of Hai-Nan Island as shown in Fig. 11.

4. Discussion

Obviously, the tidal wave propagates into the Gulf of Tongking mainly through the southern open boundary. The tidal amplitude

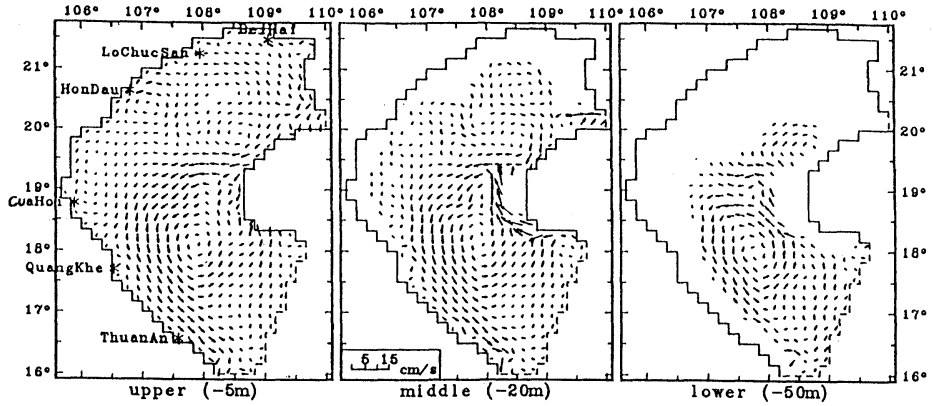

Fig. 10. The calculated residual flow chart caused by K_1 tide at three layers.

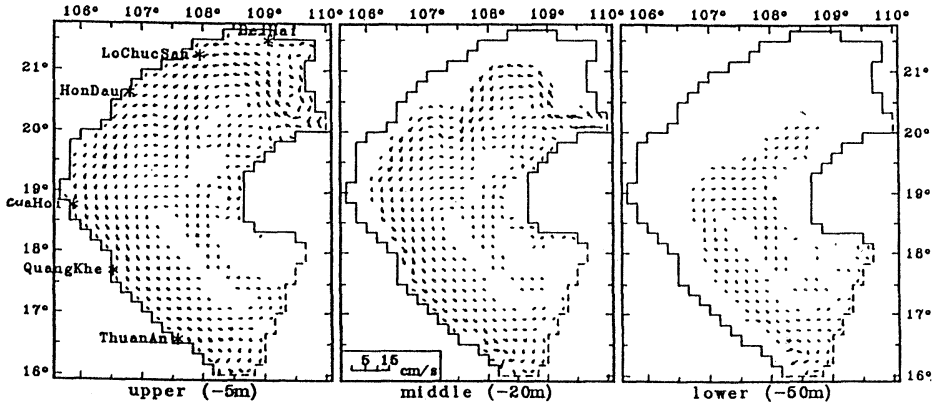

Fig. 11. The calculated residual flow chart caused by M_2 tide at three layers.

is increased due to decreasing of the water volume. On the other hand, the wave is reflected by the shore line and this process is repeated complicatedly in a semi-closed sea area as the Gulf of Tongking. Therefore, the tidal amplitude is the highest at the head of the gulf and this part of the shore line plays the most important role in the wave reflection. As a result, an amphidromic point of the diurnal tidal wave of K_1 and O_1 exists in the coastal zone of Thuan-An. In other word, the incident wave amplitude is canceled by the reflected one there. In the cases of the semi-diurnal waves, whose wave lengths are about 1/2 of the diurnal ones, there is no amphidromic point. However, a smaller amplitude region appears in the coastal zone of Hon-Dau, i.e. about a half of the distance from Thuan-An to the head of the gulf, because in this region the tidal amplitude is influenced strongly by other different parts of the shore line as well as the Hai-Nan Strait.

The horizontal distribution of tidal type $F\left(=\frac{H_{K1}+H_{O1}}{H_{M2}+H_{S2}}\right)$ obtained from the numerical model is drawn in Fig. 12. It shows that nearly in the whole gulf, except near Thuan-An, the tidal type is diurnal($F>1.25$). The remarkable amplitude increase of the diurnal tides in comparison with the semidiurnal ones during propagating in the gulf is due to the resonant phenomenon. This is suitable to the results of a study on natural oscillation of the Gulf of Tongking (NINH and DUYET 1995): one of the natural oscillating periods of the Gulf of Tongking is about 19.6 hours, i. e. near the diurnal period.

In this model a horizontal grid size of about 18km is used, therefore it is impossible to include the local topography effects in detail. The obtained results show that the calculated

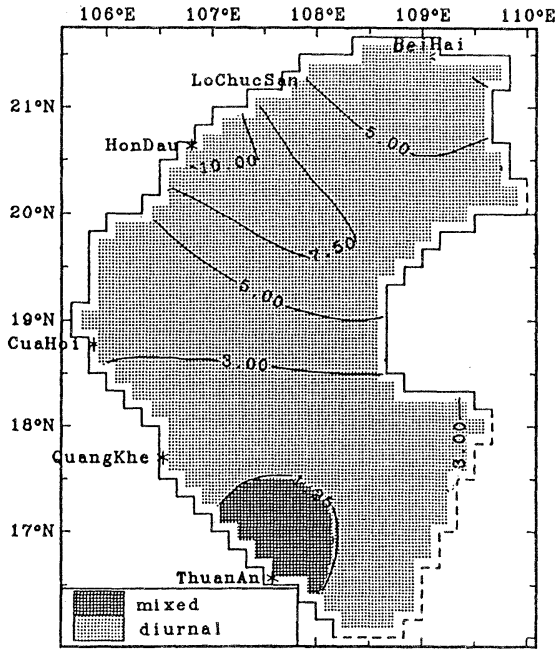

Fig. 12. The horizontal distribution of tidal type $F=(H_{K1}+H_{O1})/(H_{L2}+H_{S2})$.

results at some stations are worse than at others, for example, at Lo-Chuc-San. One of reasons may be the complication of local topography. Because of the lack of tidal current information, the tidal currents are assessed in only quantity. However, on the basis of the obtained results it can be said that the model simulates well the main characteristics of tidal process in the Gulf of Tongking.

In this study the TOPEX data are exploited. Therefore, the calculated results are verified not only at the tide gauge stations but also at some offshore points. Furthermore, the 3-D structure of tidal currents are taken into account. These have not been considered in the former studies (THUY, 1969, HUANG *et al.*, 1994) yet.

5. Conclusion

The 3-D numerical model of tide and tidal currents in the Gulf of Tongking is established. The obtained results are as follows.

1-The co-range and co-phase charts of 4 major constituents K_1, O_1, M_2, S_2 are reproduced well. As a result, the chart of tidal type is drawn. It shows that the tidal type in the gulf is diurnal, except near Thuan-An.

2-The 3-D characteristics of tidal current in the gulf are simulated. The predominant direction of tidal currents is parallel to the shore. The strongest currents occur in the south-west coastal zone of Hai-Nan. This agrees well with the observed data in quantity.

3-The tide-induced residual flows due to K_1 and M_2 tidal components are calculated.

Acknowledgments

The authors express their sincere thanks to Mr. T. TAKAO who prepared and processed observed data in order to calibrate the numerical model, to Mr. X. GUO who had useful discussion, and to other colleagues at Coastal Oceanography Laboratory of Ehime University for their help during this study.

References

FANG, G. H. (1986) : Tide and tidal current charts for the marginal seas adjacent to China, Chin. J. of Oceanology and Limnogy **4**(1), 1-16.

HUANG, O. Z, W. Z, WANG and J. C. CHEN(1994) : Tides, tidal currents and storm surge set-up of South China Sea. In "Oceanology of China Seas", edited by ZHOU D. et al., Kluwer Academic Publishers, 113-122.

LARDNER, R. W. (1988) : A new algorithm for three dimensional tidal and storm surge computations, App. Math. Modeling, Vol. 12, 471-480.

NIHOUL, J. C. J and B. M. JAMART(1987) : Three-dimensional models of marine and estuarine dynamics, Elsevier Science Publishers B. V, 35-54, 245-268.

NINH P. V and T. T. N. DUYET(1995) : Natural oscillation of the semi-closed bays, Proceedings of the 4th National Conference on Fluid Mechanics, Hanoi, 12. 1995.

RAMMING H. G. and Z. KOWALIK(1980) : Numerical modeling of marine hydrodynamics, Elsevier Scientific Publishing Company, 112-164.

THUY, N. N. (1969) : Some peculiarities of the formation of tidal phenomena i the South China Sea, Okeanologia **9**(2), 235-249.

YANAGI, T.,T. TAKAO and A. MORIMOTO(1997) : Cotidal and co-range charts in South China Sea derived from satellite altimetry, in press).

Received August 30, 1996
Accepted December 20, 1997